JOURNAL OF NANO- AND ELECTRONIC PHYSICS
Vol. 12 No 3, 03029(4pp) (2020)
ЖУРНАЛ НАНО- ТА ЕЛЕКТРОННОЇ ФІЗИКИ
Том 12 № 3, 03029(4cc) (2020)

Hopping Conductivity Mechanism in Cd_3As_2 Films Prepared by Magnetron Sputtering

V.S. Zakhvalinskii[1], E.A. Pilyuk[1,*], T.B. Nikulicheva[1], S.V. Ivanchikhin[1], M.N. Yaprintsev[1], I.Yu. Goncharov[1,2], D.A. Kolesnikov[1], A.A. Morocho[1], O.V. Glukhov[3]

[1] *Belgorod National Research University, 85, Pobedy St., 308015 Belgorod, Russia*
[2] *Belgorod State Technological University Named After V.G. Shukhov, 46, Kostyukova St., 308012 Belgorod, Russia*
[3] *National University of Radioelectronics, 14, Science Boulevard, 61166 Kharkiv, Ukraine*

(Received 07 March 2020; revised manuscript received 15 June 2020; published online 25 June 2020)

Cadmium arsenide films on oxidized silicon substrates were obtained by RF magnetron sputtering. The structure and morphology of the surface were studied by atomic force microscopy (AFM) and Raman spectroscopy (RS). The Raman spectrum contains peaks characteristic for Cd_3As_2 films at 194, 249, and 303 cm^{-1}. The carrier mobility in the samples was $0.15\text{-}1.7 \cdot 10^3$ $cm^2V^{-1}s^{-1}$ at concentrations of $0.7\text{-}4.4 \cdot 10^{19}$ cm^{-3}. It has been established that for the sample No 1 in the temperature range T = 10-15 K, the variable-range hopping (VRH) conductivity mechanism according to the Mott law is implemented. This can be explained by the fact that a microscopic disorder becomes important for electron localization in this temperature region. This is due to a decrease in temperature or an increase in the degree of disorder. In this case, the jump becomes possible only inside the Mott energy band near the Fermi level. The charge transfer in sample No 2 at T = 220-300 K is carried out by the VRH conductivity of the jump over localized states lying in a narrow energy band near the Fermi level. These states can be created by grain boundaries and dislocations. The relations between the values of the Coulomb gap Δ and the zone width of localized states W are consistent with the corresponding conduction mechanism.

Keywords: Cadmium arsenide, Dirac semimetals, Thin films, Hopping conductivity.

DOI: 10.21272/jnep.12(3).03029 PACS numbers: 68.37. – d, 72.20. – i

1. INTRODUCTION

Dirac semimetals (DSMs) with a linear dispersion law near the Dirac points are 3D analogues of graphene [1]. Because of their characteristic quantum transport due to a nontrivial electronic structure, DSMs have attracted considerable interest. One of the most interesting properties of DSMs is the chirality of electrons, when the spins of electrons are parallel or antiparallel to the direction of their movement and, thus, form right- or left-handed chiral electrons (chiral anomaly) [2]. In addition, DSMs can be converted into a quantum spin Hall insulator with a substantial forbidden energy gap due to a decrease in dimension.

Cd_3As_2, being a typical 3D DSM is characterized by new transport phenomena, such as ultrahigh mobility, high magnetoresistance (MR), non-trivial Berry phase of Dirac fermions, and negative MR caused by a chiral anomaly. In addition, it is chemically stable under air. The mobility of carriers in Cd_3As_2, lying in the range $9 \cdot 10^6$ to $4.60 \cdot 10^7$ $cm^2V^{-1}s^{-1}$ [3, 4], is greater than in graphene and is the highest for any known bulk semiconductor.

Until recently, most magnetotransport measurements have focused on Cd_3As_2 bulk materials. However, it is no less interesting to study thin films and nanostructures that can exhibit surface phase coherent transport and quantum size effect [2], leading to Aaronov-Bohm vibrations [5] and quantum Hall isolated states [6].

Therefore, it is highly desirable to produce Cd_3As_2 thin films with excellent crystallinity for transfer studies and to develop possible optoelectronic applications using the Cd_3As_2 thin film system. Here we present a brief review of the study of Cd_3As_2 thin films obtained by magnetron sputtering.

2. EXPERIMENTAL TECHNIQUE

Cd_3As_2 films were obtained by RF magnetron sputtering at the BH-2000 under argon atmosphere at a pressure of $8 \cdot 10^{-3}$ mbar. The deposition rate at a supplied power of 10 W was about 1 nm/min. The spraying time for samples № 1 and №2 was 90 and 40 min, respectively. Oxidized silicon KDB-0.1 <100> was used as a substrate. The substrate temperature during the deposition process was 20 °C. The target, which was used as a cathode, was a polycrystalline disk with a diameter of 40 mm and a thickness of 3 mm. The Cd_3As_2 synthesis for the target was carried out by direct fusion of Cd and As in vacuum.

The morphology features of the thin layers were studied by tapping-mode AFM (NTEGRA Aura, NT-MDT).

The spectrum of Raman scattering of Cd_3As_2 films was obtained using a LabRam HR Evolution Raman spectrometer (HORIBA JOBIN YVON SAS, France) at room temperature using a laser with a wavelength of 532 nm, a power of 50 mW, and a spectral resolution of 0.5 cm^{-1}.

The transport properties were studied according to the standard six-point scheme using Janis CCS-350S helium cryostat installation in a temperature range of 10-300 K and magnetic fields of 0 and 1 T. Gold contacts for the sample were deposited by magnetron sputtering.

* pilyuk@bsu.edu.ru

 © 2020 Sumy State University

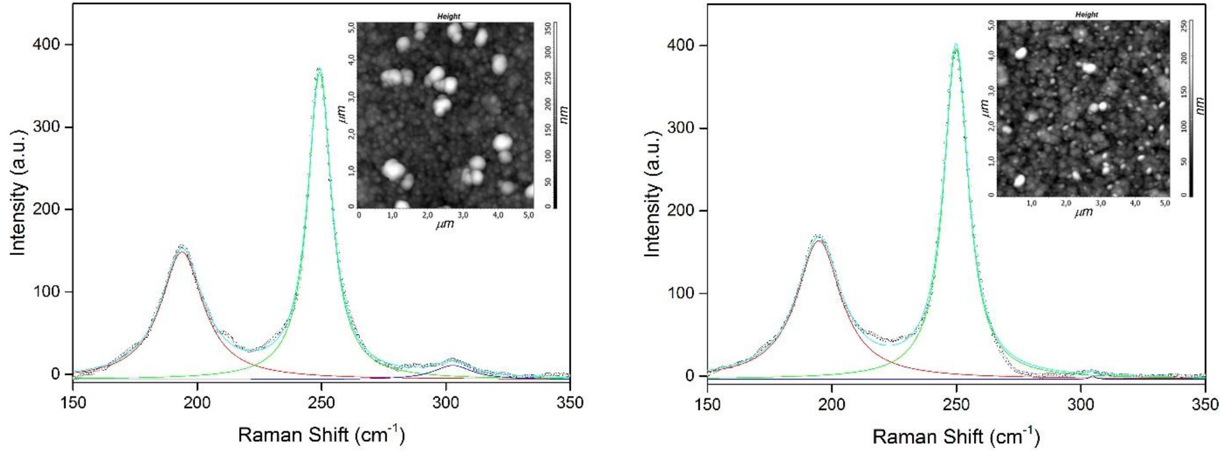

Fig. 1 – Raman spectrum and AFM results (inset) for Cd_3As_2 thin film of samples № 1 (left) and № 2 (right)

3. RESULTS AND DISCUSSION

AFM results show that the films are continuous with a granular structure with an average granule size of 143 and 117 nm for samples № 1 and № 2, respectively.

In the Raman spectrum for samples № 1 (№ 2), presented in Fig. 1, one can see two pronounced peaks at 194 and 249 cm^{-1} with full width at half maximum (FWHM) of 21 (16) and 12 (14) cm^{-1}, respectively, and a weak peak at 303 cm^{-1} with FWHM of 19 (3) cm^{-1}.

According to [7], the Raman spectrum of α-Cd_3As_2 should contain 145 active modes:

$$\Gamma^R = 26\ A_1 + 27\ B_1 + 27\ B_2 + 65\ E.$$

It is known that in the range of 100 to 400 cm^{-1} the Raman spectrum at 77 K for α-Cd_3As_2 single crystals with polarization $z\ (x+y,\ \bar{x}+y)\ \bar{z}$ has characteristic peaks at 192 and 247 cm^{-1} (symmetry $B_1 + B_2$) and a strong peak at 300 cm^{-1} (A_1) in accordance with the rules of Raman selection [8].

Peaks at 194 and 249 cm^{-1} are characteristic of Cd_3As_2 films [9]. The peak at 303 cm^{-1} can be described by a three-band model [7], according to which the incident radiation excites an electron from the valence band to a higher conduction band, and then the electron passes to the lower conduction band. The frequency with which a peak in the Raman spectrum is observed corresponds to the gap between the valence band and the lower conduction band. The first of these transitions is Σ_1–Σ_4, which explains the increase in intensity at 300 cm^{-1}, when the energy of the incident light becomes equal to 2.8 eV.

From the results of measurements of the Hall constant, the electron concentration and mobility were calculated at 10 K, being equal to $4.4 \cdot 10^{19}$ cm^{-3} and $1.7 \cdot 10^3$ cm^{2}V^{-1}s^{-1}; $0.7 \cdot 10^{19}$ cm^{-3} and $1.5 \cdot 10^2$ cm^{2}V^{-1}s^{-1} for samples № 1 and № 2, respectively.

In order to determine the mechanism of conductivity of the samples in the temperature range close to helium, the analysis of the temperature dependence of the specific resistance is carried out in accordance with [10]:

$$\rho(T) = \rho_0 \exp\left[E_A/(kT)\right], \tag{1}$$

where ρ_0 is the pre-exponential factor, E_A is the activation energy, k is the Boltzmann constant.

Fig. 2 shows the results of an experimental study of the temperature dependence of the resistivity.

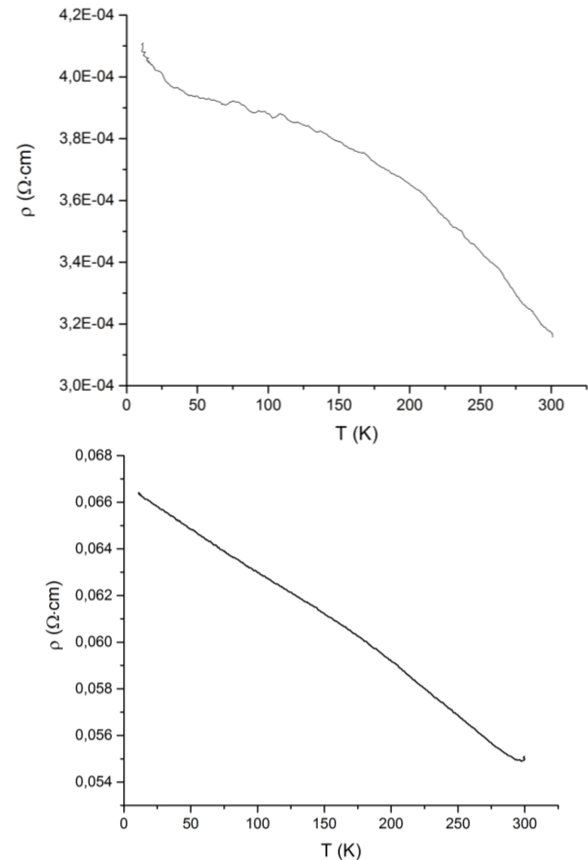

Fig. 2 – Temperature dependence of the resistivity of Cd_3As_2 thin film of samples № 1 (top) and № 2 (bottom)

Resistance analysis in the samples is carried out in accordance with the universal law:

$$\rho(T) = \rho_0 \exp\left[\left(\frac{T_0}{T}\right)^p\right] = AT^m \exp\left[\left(\frac{T_0}{T}\right)^p\right], \tag{2}$$

where T_0 is the characteristic temperature. If $p = 1$, it corresponds to the nearest-neighbor hopping conductivi-

ty (in this case, instead of T_0, the activation energy $E_0 \equiv kT_0$ is usually introduced); if $p = 1/4$, it corresponds to the Mott variable-range hopping (Mott VRH) conductivity mechanism, if $p = 1/2$ it is the Shklovsky-Efros VRH (SE VRH) [10]. The value of m is determined depending on the conduction mode and the type of wave function ψ ($\Gamma \equiv \left[kT\left(T_0/T\right)^p a/\left(2\hbar s\right)\right]^2$) of localized carriers, respectively. In equation (2), $T_0 = T_M$ or $T_0 = T_{SE}$ for $p = 1/4$ or $p = 1/2$, respectively, where

$$T_M = \frac{\beta_M}{kg(\mu)a^3},\ T_{SE} = \frac{\beta_{SE}e^2}{\kappa ka} \qquad (3)$$

κ is the dielectric constant, $\beta_M = 21$, $\beta_{SE} = 2.8$ [10].

The hopping conduction mechanism is characterized not only by the value of the parameter p in equation (2). Also, the temperature dependence of the factor at the beginning of the equation and given by the power law dependence on m is no less important. Therefore, simultaneous and independent determination of both parameters m and p is necessary. Since the local activation energy is given by $E_a \equiv d\ln\rho/d(kT)^{-1}$ [10], we can rewrite the equation (2) in the form:

$$\ln\left[E_a/(kT)+m\right] = \ln p + p\ln T_0 + p\ln(1/T). \qquad (4)$$

It can be seen that for a certain hopping conduction mode, the left side of equation (4) is a linear function of $\ln(1/T)$ for a given value of m, and the value of parameter p can be determined from the slope of the graph $\ln[E_a/(kT) + m]$ on $\ln(1/T)$ (Fig. 3).

The condition for the realization of VRH conductivity is caused by jumps between centers that have energies in a certain ε-neighborhood of the Fermi level, where there are obviously empty sites. In the implementation of Mott VRH conductivity, it is assumed that the density of states in the vicinity of the Fermi level $\mu \pm \varepsilon$ is considered constant: $g = g_\mu$. Then the number of states in this neighborhood is given by $N(\varepsilon) = g_\mu\varepsilon$, the average distance between them in the case of a thin film is $r_{i,j} \approx \left[N(\varepsilon)\right]^{-1/2}$, and the energy difference is of the order of ε.

The average change in energy during jumping for thin films is determined from the minimum condition [11]:

$$\frac{d}{d\varepsilon}U_{ij}(\varepsilon) = 0,\ \varepsilon = \varepsilon_{min} = \left(\frac{T}{g_\mu^{1/2}a_B}\right) = \left(T_M T^2\right)^{1/3},$$

and the average jump length:

$$r \approx \left(\frac{a_B}{g_\mu T}\right)^{1/3} \approx a_B\left(\frac{T_M}{T}\right)^{1/3}.$$

For sample № 1, the Mott VRH conductivity mechanism is realized in the low temperature range $T = 10$-15 K. This can be explained by the fact that microscopic disorder becomes important for electron localization, which is facilitated by a decrease in temperature or by increasing the degree of disorder. In this case, the jump becomes possible only within a limited range of energies, the so-called Mott energy band, near the Fermi level [10].

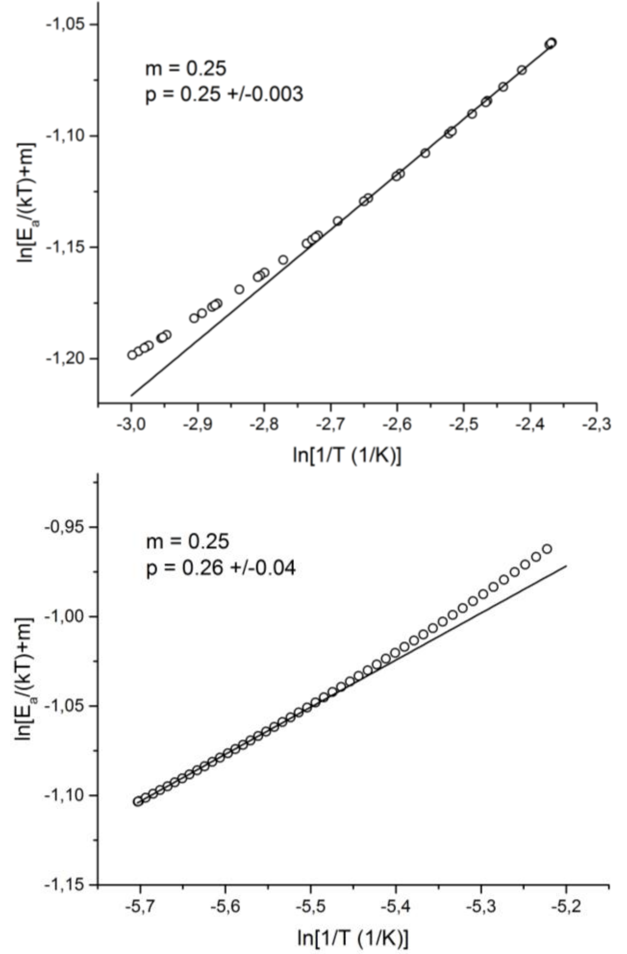

Fig. 3 – Dependence of $\ln[E_a/(kT) + m]$ on $\ln(1/T)$ of samples № 1 (top) and № 2 (bottom)

For sample № 2, the Mott VRH conductivity mechanism is realized in the high temperature range $T = 220$-300 K. This can be explained by the fact that charge transfer in the studied film is carried out by VRH of the jump over localized states lying in a narrow energy band near the Fermi level. These states can be created by extended defects – intergranular boundaries and dislocations.

All calculated parameters for samples № 1 and № 2 are presented in Table 1.

In the implementation of the SE VRH, the density of states $g(\mu)$, in contrast to the Mott VRH, is not constant due to the presence of the Coulomb gap:

$$g(\varepsilon) \propto \left(\frac{\kappa}{e^2}\right)^d |\varepsilon|^{d-1},\ g(0) = 0,$$

where d is the dimension of space, the energy ε is defined from the Fermi level.

In samples with the Mott VRH conductivity mechanism the influence of the Coulomb gap is minimal, because it is realized only at $B = 0$. Therefore, the density of localized states (DLS) in the acceptor level can be approximated by a rectangular shape, the width of the Coulomb gap in the DLS of the Fermi level is given by $W \approx kT_M^{3/4}T_0^{-1/4}$ [10]. From the expression $g(\mu) \approx N_A/(2W)$

one can obtain the concentration of acceptor centers. We can find the value of a from equation (3). The value of κ is obtained from the expression $E_A = F(K)e^2\kappa^{-1}N_A^{1/3}$, where $F(K)$ is some universal compensation function, $F(K) = 0.43$. Then, from the expression $g_0 = 3\kappa^3\Delta^2/(\pi e^6)$ [10] we find the value of Δ under the assumption that $g_0 \approx g(\mu)$. The values are shown in Table 1.

The relations between Δ and W values are consistent with the corresponding conduction mechanism at $B = 0$. The ratio $\Delta/W \sim 0.1$ is favorable for the Mott VRH conductivity mechanism.

Table 1 – Microscopic parameters for thin film samples Cd_3As_2

No	ρ, Ohm·cm	E_A, meV	T_M, K	g_μ, $cm^{-3}meV^{-1}$	ε_{min}, meV	r, nm	a, nm	κ	Δ, meV	W, meV
1	$3.95 \cdot 10^{-4}$	0.034	18.5	$9.9 \cdot 10^{15}$	19.5	2.3	12	176	$3.97 \cdot 10^{-2}$	0.36
2	5.03	2.6	1181	$1.55 \cdot 10^{14}$	77.9	6.5	12	162	2.79	8.21

4. CONCLUSIONS

RF magnetron sputtering produced cadmium arsenide films on oxidized silicon substrates. According to the AFM results, the films are continuous with a granular structure. The Raman spectrum contains peaks characteristic for Cd_3As_2 films at 194, 249, and 303 cm^{-1}. The mobility of electrons is greater in the sample № 1 and rises to $4.4 \cdot 10^{19}$ cm^{-3} with a concentration of $1.7 \cdot 10^3$ $cm^2V^{-1}s^{-1}$. The Mott VRH conductivity mechanism is realized in both samples in temperature ranges $T = 10$-15 K and $T = 220$-300 K for samples № 1 and № 2, respectively. Microscopic parameters were determined, the ratio between which is consistent with the conduction mechanism for the obtained samples.

ACKNOWLEDGEMENTS

The work was supported by the Russian Science Foundation, Grant No. 19-79-00152.

REFERENCES

1. M.Z. Hasan, C.L. Kane, *Rev. Mod. Phys.* **82**, 3045 (2010).
2. Y.-K. Yang, F.-X. Xiu, F.-Q. Wang, J. Wang, Y. Shi, *Chin. Phys. B* **28**, 107502 (2019).
3. T. Liang, Q. Gibson, M.N. Ali, M. Liu, R.J. Cava, N.P. Ong, *Nature materials* **14** 280 (2015).
4. Y. Zhao, H. Liu, C. Zhang, H. Wang, J. Wang, Z. Lin, Y. Xing, H. Lu, J. Liu, Y. Wang, S.M. Brombosz, Z. Xiao, S. Jia, X.C. Xie, J. Wang, *Phys. Rev. X* **5**, 031037 (2015).
5. L.-X. Wang, C.-Z. Li, D.-P. Yu, Z.-M. Liao, *Nat. Commun.* **7**, 10769 (2016).
6. Z. Wang, H. Weng, Q. Wu, X. Dai, Z. Fang, *Phys. Rev. B* **88**, 125427 (2013).
7. A. Sharafeev, V. Gnezdilov, R. Sankar, F. C. Chou, and P. Lemmens, *Phys. Rev. B* **95**, 235148 (2017).
8. P. Schönherr, T. Hesjedal *Appl. Phys. Lett.* **106**, 013115 (2015).
9. A.V. Suslov, A.B. Davydov, L.N. Oveshnikov, L.A. Morgun, K.I. Kugel, V.S. Zakhvalinskii, E.A. Pilyuk, A.V. Kochura, A.P. Kuzmenko, V.M. Pudalov, B.A. Aronzon, *Phys. Rev. B* **99**, 094512 (2019).
10. R. Laiho, A.V. Lashkul, K.G. Lisunov, E. Lähderanta, M.A. Shakhov, V.S. Zakhvalinskii, *J. Phys. Condens. Matter* **20**, 295204 (2008).
11. V.F. Gantmakher, *Elektrony v neuporyadochennykh sredakh*, 288 (M.: FIZMATLIT: 2013) [In Russian].

Механізм стрибкової провідності в плівках Cd_3As_2, отриманих магнетронним розпиленням

В.С. Захвалінскій[1], Е.А. Пилюк[1], Т.Б. Никуличева[1], С.В. Іванчіхін[1], М.Н. Япринцев[1], І.Ю. Гончаров[1,2], Д.А. Колесніков[1], А.А. Морочо[1], О.В. Глухов[3]

[1] *Белгородський державний національний дослідницький університет, вул. Перемоги, 85, 308015 Белгород, Росія*

[2] *Белгородський державний технологічний університет імені В.Г. Шухова, вул. Костюкова, 46, 308012 Белгород, Росія*

[3] *Національний університет радіоелектроніки, бульвар Науки, 14, 61166 Харків, Україна*

Плівки арсеніду кадмію на підкладках окисленого кремнію отримані ВЧ-магнетронним розпиленням. Досліджено структуру та морфологію поверхні методами АСМ та раманівської спектроскопії. На спектрі КРС присутні характерні для плівок Cd_3As_2 піки при 194, 249 і 303 $см^{-1}$. Рухливість носіїв в зразках склала 0,15-1,7 $\cdot 10^3$ $см^2В^{-1}с^{-1}$ при концентрації 0,7-4,4 $\cdot 10^{19}$ $см^{-3}$. Встановлено, що для зразка №1 в інтервалі температур $T = 10 \div 15$ К реалізується механізм електропровідності за законом Мотта. Це можна пояснити тим, що мікроскопічне розупорядкування стає важливим для локалізації електронів в цьому температурному регіоні. Цьому сприяє зниження температури або зростання ступеня безладу. В цьому випадку стрибок стає можливим тільки всередині енергетичної смуги Мотта поблизу рівня Фермі. Перенесення заряду в зразку №2 при $T = 220 \div 300$ К здійснюється шляхом стрибкової провідності електронів зі змінною довжиною стрибка по локалізованим станам, що лежать у вузькій смузі енергій поблизу рівня Фермі. Ці стани можуть створюватися міжзеренними межами і дислокаціями. Співвідношення між значеннями кулонівської щілини Δ і шириною зони локалізованих станів W узгоджуються з відповідним механізмом провідності.

Ключові слова: Арсенід кадмію, Діраковскі напівметали, Тонкі плівки, Стрибкова провідність.